

Towards Adversarial-Resilient Deep Neural Networks for False Data Injection Attack Detection in Power Grids

Jiangnan Li*, Yingyuan Yang[§], Jinyuan Stella Sun*, Kevin Tomsovic*, Hairong Qi*

*The University of Tennessee, Knoxville, jli103@vols.utk.edu, {jysun, tomsovic, hqi}@utk.edu

[§]University of Illinois Springfield, yyang260@uis.edu

Abstract—False data injection attack (FDIA) is a critical security issue in power system state estimation. In recent years, machine learning (ML) techniques, especially deep neural networks (DNNs), have been proposed in the literature for FDIA detection. However, they have not considered the risk of adversarial attacks, which were shown to be threatening to DNN’s reliability in different ML applications. In this paper, we evaluate the vulnerability of DNNs used for FDIA detection through adversarial attacks and study the defensive approaches. We analyze several representative adversarial defense mechanisms and demonstrate that they have intrinsic limitations in FDIA detection. We then design an adversarial-resilient DNN detection framework for FDIA by introducing random input padding in both the training and inference phases. Extensive simulations based on an IEEE standard power system show that our framework greatly reduces the effectiveness of adversarial attacks while having little impact on the detection performance of the DNNs.

Index Terms—false data injection attack, adversarial machine learning, adversarial defense, smart grid

I. INTRODUCTION

State estimation is a core application in the power grids control center. The analog measurements and status data from remote sensors are received by the state estimator to determine the network topology and best estimates of the voltage, current magnitudes and phase (i.e., system state). Meanwhile, a built-in residue-based bad data detection mechanism is employed by the state estimator to remove bad data and filter measurement errors. Operators and advanced applications receive the refined data to compute market prices and make operational decisions.

False data injection attack (FDIA) was proposed by Liu *et al.* in 2009 [1]. It enables attackers to inject malicious false data into legitimate measurements while bypassing the bad data detection, causing the estimator to output incorrect system states. These attacks can disturb critical operations, such as contingency analysis, that rely on the estimated state. Since then, various FDIAs have been developed, such as FDIA with incomplete information [2], blind FDIA [3], and outage masking [4].

As FDIA poses a serious threat to the security of power grids, various detection methods were proposed in the literature, such as basic measurement protection [5] and detection with phasor measurement units (PMU) [6]. In recent years, machine learning (ML), especially deep neural network (DNN), becomes a key technique to detect FDIA in the

literature [7]–[15]. The basic system architecture of DNN-based FDIA detection is shown in Fig. 1. DNNs take advantage of the statistical properties of measurement data in a power system and can achieve state-of-the-art detection performance. Moreover, they are usually pure software systems and can be deployed in the control center without additional equipment or infrastructure upgrades, making them ideal defense techniques against FDIA.

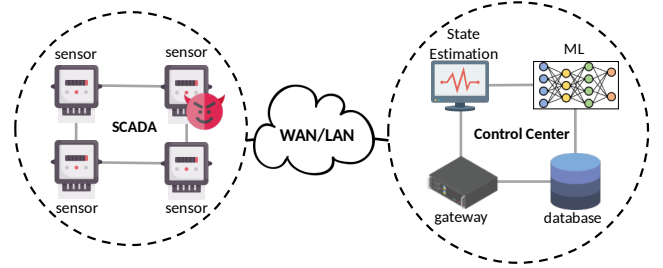


Fig. 1: Illustration of DNN-based FDIA detection. The attacker is assumed to compromise a subset of the sensors and inject false data. A trained DNN is placed in the control center to detect and remove malicious measurements.

However, research in the artificial intelligence (AI) domain has demonstrated that the well-performed DNNs are highly vulnerable to adversarial attacks. By adding well-crafted perturbations to the DNN’s input, the attacker can deceive the DNN to output wrong decisions. Recent research has shown that such attacks are also effective on power system applications [16]–[19], including DNN-based FDIA detection [20] and state estimation [21]. Therefore, the risks of adversarial attacks need to be considered and more robust DNNs that are resilient to adversarial attacks should be proposed for FDIA detection in power system state estimation. However, the state-of-the-art approaches to mitigate adversarial attacks, such as adversarial detection and adversarial training, are mainly designed for computer vision applications and make specific assumptions that are not applicable to FDIA detection. For example, adversarial detection approaches assume that adversarial examples follow a different distribution from normal inputs and train an auxiliary DNN to distinguish adversarial examples before forwarding them to the functional DNN [22]. However, as shown in this paper, such assumptions become infeasible in FIDA detection due to the constraints from the

physical systems. There is currently a lack of research on effectively mitigating adversarial attacks in DNN-based FDIA detection.

In this work, we study the defense mechanisms to mitigate adversarial attacks in DNN-based FDIA detection. We evaluate three state-of-the-art defense methods and show that they have intrinsic limitations on adversarial prevention in FDIA detection. We then propose a general random input padding framework for DNN-based FDIA detection. Our framework can be easily adapted to the different ML models in the existing research [7]–[15] with basic changes to configurations in the training process and detection deployment. We evaluate our approach with synthetic datasets generated from the IEEE standard 118-bus system. The result shows that the proposed framework can significantly mitigate adversarial attacks. Our main contributions include:

- We highlight the need for robust DNN-based methods that are resilient to adversarial attacks and summarize the adversarial defense properties and requirements in FDIA detection.
- Three typical adversarial defense approaches are evaluated, including defensive distillation, adversarial training, and adversarial detection. We demonstrate that they are not capable of mitigating adversarial attacks in FDIA detection via analysis and simulations.
- We propose a general defense framework that randomly pads the model input in both training and testing stages. The framework decreases the effectiveness of adversarial perturbations and can be seamlessly adapted to DNNs proposed in the literature.
- We conduct our simulations based on the standard IEEE 118-bus power system. The simulation result shows that our framework can effectively mitigate adversarial attacks while inducing little degradation in the models' detection accuracy of normal inputs.

The rest of the paper is organized as follows. The related work is presented in Section II. We cover background information on state estimation and FDIA in Section III. Section IV presents the adversarial attacks in DNN-based FDIA detection. We discuss the limitations of the existing defense approaches and propose our framework in Section V. Simulation results are presented in Section VI. Section VII discusses the limitations and future work. Finally, Section VIII concludes the paper.

II. RELATED WORK

A. FDIA Detection

FDIA was firstly proposed by Liu *et al.* in 2009 [1], their work showed that if an attacker can compromise a certain number of sensor measurements and have the knowledge of the \mathbf{H} matrix, she/he can always generate a false data vector that can bypass the residual-based bad data detection scheme that was integrated with state estimation. After that, [2] loosed the attack constraints and claimed that the attacker can launch FDIA even with incomplete information of \mathbf{H} . Another variant is the blind FDIA presented by Yu and Chin [3] who utilized

principal component analysis (PCA) to generate an estimated PCA matrix.

Since FDIA is considered as a serious threat to power system security, many following studies and countermeasures are proposed. [23] analyzed the impact of FDIA with static security assessment and claimed that FIDA can deceive the operator to make wrong actions, such as load shedding. Khalaf *et al.* studied and evaluated FDIA under wide area protection settings and showed that the FDIA can affect the grids' operation and stability [24]. FDIA requires the attacker to compromise a certain number of measurements. If enough measurements are well-prevented, the system will be guaranteed to be secure from FDIA, as demonstrated in [25]. Bi and Zhang utilized graph theory to locate the meters to be protected [26]. Some studies took advantage of new hardware devices, such as PMUs. The PMUs' measurements are synchronized to GPS signals and will increase the barrier for FDIA attacks. [27] and [28] investigated the placement strategies of PMUs.

The previous defense approaches either require additional hardware or extra labor to re-deploy sensors. In recent years, detection that utilized ML techniques became popular in the literature. In 2016, Ozay *et al.* first utilized ML techniques to detect FDIA [7]. They evaluated the detection performance of traditional ML algorithms such as K-Nearest Neighbour (KNN), support vector machine (SVM), and Sparse Logistic Regression (SLR) and demonstrated that ML achieved convincing detection accuracy with fine-tuned parameters. After that, Yan *et al.* studied the performance of a supervised learning classifier on detecting both direct and stealth FDIA [8]. He *et al.* employed deep learning (DL) for FDIA and electricity theft detection [9]. In 2018, [13] evaluated the performance of plain DNN in FDIA attacks. Thereafter, different DNNs were designed. The studies in [10]–[12] used recurrent neural networks (RNNs) for FDIA detection, they evaluated the DNNs with different scale power systems and all achieves high detection results. Niu *et al.* designed a DNN that adopted both convolutional neural network (CNN) and RNN to detect FDIA in dynamic time-series measurement data [14]. The false data usually follows a different distribution with legitimate data. Wang *et al.* trained an auto-encoder with pure normal measurement data and employed the reconstruction loss as the metric for FDIA detection [15]. More related work of FDIA and detection can be found in [29] and [30].

B. Adversarial Attacks

Although DNNs obtained outstanding performance in FDIA detection, they are far from reliable to be deployed in critical infrastructures like power system. Recent research in the AI domain has demonstrated that DNNs are vulnerable to adversarial attacks. In 2013, adversarial examples to DNNs were discovered by Szegedy *et al.* [31]. By adding a small crafted perturbation to the legitimate inputs, the DNNs will be led to output wrong results. Meanwhile, the same perturbation is shown to be effective to different DNNs, which is called the transferability of adversarial examples. After that, different adversarial attack algorithms were proposed. Goodfellow *et al.* presented the Fast Gradient Sign Method (FGSM) that

utilized the signed gradient values to generate perturbations [32]. After that, the Fast Gradient Method by Rozsa *et al.* used the gradient values directly [33]. Other well-known adversarial attack algorithms include the DeepFool [34] and iterative attack [35].

The potential threat of adversarial attacks to critical infrastructures also draws attention in recent research. In 2018, Chen *et al.* investigated the effect of adversarial examples with both categorical and sequential applications in power systems [16]. They then designed adversarial attacks to regression models used for load forecasting [17]. Tian *et al.* extended [16] and proposed an adaptive normalized attack for power system ML applications [18]. [20] proposed constrained adversarial machine learning in CPS applications, and demonstrated an attacker can generate adversarial examples that meet the intrinsic constraints defined by physical systems, such as the residual-based detection in state estimation.

The defense methods against adversarial attacks draw attention in both security and AI communities. The state-of-the-art defense approaches include model distillation [36], adversarial detection [22], [37], [38], adversarial training [35], [39], [40], input reconstruction [41][42], stochastic methods [42][43], and so on. More related work about adversarial attacks and defense can be found in [44].

III. TECHNICAL BACKGROUND

A. Power System State Estimation

Enabled by the supervisory control and data acquisition (SCADA) techniques, power systems utilize state estimation to estimate the state of each bus, such as voltage angles and magnitudes, through analyzing the other measurements, such as the power of transmission lines, from the remote meters. We denote the vector of state variables as $\mathbf{x} = [x_1, x_2, \dots, x_n]^T$, and the meters' measurements vector as $\mathbf{z} = [z_1, z_2, \dots, z_m]^T$. The general state estimation process can be represented as follow:

$$\mathbf{z} = \mathbf{h}(\mathbf{x}) + \mathbf{e} \quad (1)$$

where \mathbf{e} is the measurement error vectors and \mathbf{h} is a function of \mathbf{x} . In practice, a DC power flow state estimation is usually used to decrease the process time cost. A DC model can be represented as equation (2).

$$\mathbf{z} = \mathbf{H}\mathbf{x} + \mathbf{e} \quad (2)$$

The matrix $\mathbf{H}_{m \times n}$ is determined by the configurations, topology and physical parameters of the power system.

In general, a weighted least squares estimation (WLS) approach is used to solve equation (2). The estimated state vector $\hat{\mathbf{x}}$ can then be computed through equation (3):

$$\hat{\mathbf{x}} = (\mathbf{H}^T \mathbf{W} \mathbf{H})^{-1} \mathbf{H}^T \mathbf{W} \mathbf{z} \quad (3)$$

where matrix \mathbf{W} is the covariance matrix of the meters' statistical measurement errors.

In practice, \mathbf{z} may contain bad measurements due to meter errors or cyber attacks. Therefore, state estimation integrates

with a linear residual-based detection approach to remove faulty measurements according to the difference between \mathbf{z} and $\mathbf{H}\hat{\mathbf{x}}$. If the L_2 -Norm of $\|\mathbf{z} - \mathbf{H}\hat{\mathbf{x}}\|$ is larger than a threshold τ that is selected according to a false alarm rate, the measurement \mathbf{z} will be considered as polluted and be removed.

B. False Data Injection Attack

The FDIA enables an attacker to generate a false measurement vector $\mathbf{a} = [a_1, a_2, \dots, a_m]^T$ to be added to legitimate \mathbf{z} , so that the polluted measurements will be $\mathbf{z}_a = \mathbf{z} + \mathbf{a}$. [1] shows that if the attacker knows \mathbf{H} , she/he can construct $\mathbf{a} = \mathbf{H}\mathbf{c}$ (\mathbf{c} represents the estimation error) that can bypass the fault detection in state estimation, as shown by equation (4), where $\hat{\mathbf{x}}_{bad}$ and $\hat{\mathbf{x}}$ denote the estimated \mathbf{x} using \mathbf{z}_a and \mathbf{z} respectively.

$$\|\mathbf{z}_a - \mathbf{H}\hat{\mathbf{x}}_{bad}\| = \|\mathbf{z} + \mathbf{a} - \mathbf{H}(\hat{\mathbf{x}} + \mathbf{c})\| \quad (4a)$$

$$= \|\mathbf{z} - \mathbf{H}\hat{\mathbf{x}} + (\mathbf{a} - \mathbf{H}\mathbf{c})\| \quad (4b)$$

$$= \|\mathbf{z} - \mathbf{H}\hat{\mathbf{x}}\| \leq \tau \quad (4c)$$

Meanwhile, equation (5) from [1] provides an efficient way to generate a valid vector \mathbf{a} , where $\mathbf{P} = \mathbf{H}(\mathbf{H}^T \mathbf{H})^{-1} \mathbf{H}^T$ and matrix $\mathbf{B} = \mathbf{P} - \mathbf{I}$.

$$\mathbf{a} = \mathbf{H}\mathbf{c} \Leftrightarrow \mathbf{P}\mathbf{a} = \mathbf{P}\mathbf{H}\mathbf{c} \Leftrightarrow \mathbf{P}\mathbf{a} = \mathbf{H}\mathbf{c} \Leftrightarrow \mathbf{P}\mathbf{a} = \mathbf{a} \quad (5a)$$

$$\Leftrightarrow \mathbf{P}\mathbf{a} - \mathbf{a} = \mathbf{0} \Leftrightarrow (\mathbf{P} - \mathbf{I})\mathbf{a} = \mathbf{0} \quad (5b)$$

$$\Leftrightarrow \mathbf{B}\mathbf{a} = \mathbf{0} \quad (5c)$$

Equation (5c) indicates that \mathbf{a} is a solution of the homogeneous equation $\mathbf{B}\mathbf{X} = \mathbf{0}$. If an attacker compromised k measurements in \mathbf{z} , and there will be k non-zero elements in \mathbf{a} . Equation (5c) will then become:

$$\mathbf{B}'\mathbf{a}' = \mathbf{0} \quad (6)$$

where $\mathbf{B}'_{m \times k}$ and $\mathbf{a}'_{m \times k}$ are corresponding columns and rows sampled from \mathbf{B} and \mathbf{a} respectively according to the k compromised measurements. [1] proves that as long as $k > m - n$, non-zero \mathbf{a} always exists.

IV. ADVERSARIAL ATTACK IN FDIA DETECTION

A. Attack Properties

In this paper, we mainly consider supervised learning techniques for FDIA detection as they are more popular in the literature [7]–[14]. We note that our method can be easily extended to unsupervised learning approaches, such as the autoencoder used in [15], by designing corresponding loss functions.

Without loss of generality, we consider the DNN-based FDIA detection as a binary classification problem. The trained DNN $F : \mathbf{Z} \rightarrow Y$ maps the input measurement vectors \mathbf{Z} to their labels Y . An ideal DNN will map a legitimate measurement \mathbf{z} to legitimate label Y_0 and a false measurements $\mathbf{z}_a = \mathbf{z} + \mathbf{a}$ to false label Y_1 .

TABLE I: Terminologies and Notations

Terminology	Notation	Explanation
legitimate measurements	\mathbf{z}	sensors' original measurements
injected false data	\mathbf{a}	meets constraint $\mathbf{B}\mathbf{a} = \mathbf{0}$
false measurements	\mathbf{z}_a	$\mathbf{z}_a = \mathbf{z} + \mathbf{a}$
adversarial perturbation	\mathbf{v}	perturbation for \mathbf{z}_a
total injected false data	$\hat{\mathbf{a}}$	$\hat{\mathbf{a}} = \mathbf{a} + \mathbf{v}$, $\mathbf{B}\hat{\mathbf{a}} = \mathbf{0}$
adversarial measurements	\mathbf{z}_{adv}	$\mathbf{z}_{adv} = \mathbf{z}_a + \mathbf{v} = \mathbf{z} + \hat{\mathbf{a}}$

The adversarial attack in FDIA detection is a false-negative attack that deceive F to classify the false measurements as legitimate. The attacker needs to generate an adversarial perturbation vector \mathbf{v} and add it to the false measurement vector \mathbf{z}_a , so that the adversarial measurement $\mathbf{z}_{adv} = \mathbf{z}_a + \mathbf{v} = \mathbf{z} + \mathbf{a} + \mathbf{v} = \mathbf{z} + \hat{\mathbf{a}}$ can be classified as legitimate measurements (with Y_0 label) by F , where $\hat{\mathbf{a}} = \mathbf{a} + \mathbf{v}$ is the total injected false data. Meanwhile, the attacker requires $\hat{\mathbf{a}}$ also meet the constraint $\mathbf{B}\hat{\mathbf{a}} = \mathbf{0}$ defined by (5c) to avoid being removed by the state estimation residual-based detection system. Therefore, the adversarial measurements in FDIA detection can also be considered as special false measurements. To be clear, Table I summarizes the terminologies and notations.

B. Defense Requirements & Threat Model

White-box adversarial attacks allow the attacker to have access to the target DNN, which is a common setting in previous literature and has been extensively studied since it helps researchers to learn the weakness of DNNs more directly [44]. Robust against white-box adversarial attacks is the desired property that the DNNs should maintain [40], especially for critical infrastructure like power grids. In particular, the cyberattacks targeting power systems are usually nationwide and the attacker owns considerable resources, like the well-known Ukraine power grid attack in 2015 [45]. In this paper, we expect the defense mechanisms in DNN-based FDIA detection to be resilient to white-box adversarial attacks.

Based on the attack requirements described in [1], from the attacker's point of view, we summarize the threat model of the adversarial attacks in FDIA detection:

- The attacker can compromise k ($k > m - n$) measurements in the power system and freely modify the compromised measurements. In practice, this can be completed by physical penetration to the sensors or compromise the communication networks. For example, the IEEE C37.118 communication protocol [46] used in smart grids does not have necessary security mechanisms, and the attacker who compromises can access the measurement data directly.
- As described in [1], the attacker knows the \mathbf{H} matrix to launch FDIA.
- We study a white-box adversarial attack, and the total injected false data $\hat{\mathbf{a}}$ should always follow $\mathbf{B}\hat{\mathbf{a}} = \mathbf{0}$ to bypass the built-in residual-based detection mechanism in state estimation.

C. Adversarial Attack Algorithm

Notation: To describe the algorithm, if $A = [a_0, a_1, \dots, a_{m-1}]$ is a vector and $B = [b_0, b_1, \dots, b_{n-1}]$ is an index vector of A ($0 < n \leq m$), we will use $A_B = [a_{b_0}, a_{b_1}, \dots, a_{b_{n-1}}]$ to denote the sampled vector of A according to vector B .

The algorithms to generate adversarial measurements can be different and dependent on specific applications. The state-of-the-art adversarial attack algorithms include L-BFGS [31], FGSM [32], DeepFool [34], BIM [35], JSMA [47], PGM [48], C&W [49] and so on. All of them utilize gradient-based methods to search for adversarial perturbations for the given inputs. In this paper, we employ the iterative projection framework in [35] and [48] since the adversarial perturbation \mathbf{v} needs to follow the constraints defined by the power system. However, instead of projecting to the ε -neighbor ball as in [35] and [48], the attacker needs to map the adversarial perturbation \mathbf{v} to the solution space of the homogeneous equation $\mathbf{B}\mathbf{v} = \mathbf{0}$, so that the total injected false data $\mathbf{B}\hat{\mathbf{a}} = \mathbf{B}(\mathbf{a} + \mathbf{v}) = \mathbf{B}\mathbf{a} + \mathbf{B}\mathbf{v} = \mathbf{0}$ and will enable the adversarial measurements \mathbf{z}_{adv} to bypass the residual-based detection. We denote the index of the compromised k measurements in \mathbf{z} as C and the uncompromised as U . The algorithm we use to attack DNN in FIDA detection can be described in Algorithm 1, which uses an iterative search for adversarial example generation.

Algorithm 1: Adversarial Attacks in FDIA

```

1 Input:  $F, C, \mathbf{z}_a, size, \mathbf{B}', Y_1$ 
2 Output:  $\mathbf{v}$ 
3 function genPer( $F, C, \mathbf{z}_a, size, \mathbf{B}', Y_1$ )
4   initialize  $\mathbf{v} = 0$ 
5   while  $F(\mathbf{z}_a + \mathbf{v})$  equals  $Y_1$  do
6     calculate gradient  $G = \nabla_{\mathbf{z}_a + \mathbf{v}} L(F(\mathbf{z}_a + \mathbf{v}), Y_1)$ 
7     set all elements of  $G_U$  in  $G$  to zero
8     define  $G' = G_C$ 
9     project  $G'$  to the solution space of  $\mathbf{B}'G' = \mathbf{0}$ 
10     $\epsilon = size / \max(\mathbf{abs}(G'))$ 
11     $\mathbf{r} = \epsilon G$ 
12    update  $\mathbf{v} = \mathbf{v} + \mathbf{r}$ 
13  end
14  return  $\mathbf{v}$ 
15 end

```

As shown by Line 9 in Algorithm 1, the attacker projects the adversarial perturbation to the solution space of the constraint matrix. In this paper, we employ the dependent variable scheme in [20] to implement the projection. Given the constraint matrix \mathbf{B}' , we first obtain the corresponding independent variable index I , dependent variable index D , and their dependency matrix \hat{B} . In each iteration, we will keep the gradient values of the independent variable (G'_I), and the values of the dependent measurements (G'_D) are calculated from G'_I based on their correlation $G'_D = \hat{B}G'_I$. This projection process will force \mathbf{v} to follow the constraint $\mathbf{B}\mathbf{v} = \mathbf{0}$. Algorithm 1 finally generates \mathbf{v} that deceives the model F to classify $\mathbf{z}_a + \mathbf{v}$ as legitimate.

A practical power system usually holds a constant data sampling period. For example, the sampling period of a

traditional SCADA system is around 2 to 4 seconds. The recently developed PMUs maintain a relatively higher data reporting rate (from 10Hz to 60 Hz) [46]. An adversarial attack is required to be finished within a sampling period of the target power system, but the loop (Line 5) in Algorithm 1 may keep executing. In our simulations, we will return \mathbf{v} when the cycling number reaches a threshold.

V. ADVERSARIAL DEFENSE IN FDIA DETECTION

The arms race between adversarial attacks and defense in the AI domain is still in progress. In recent years, different adversarial defense mechanisms are proposed in the literature, such as model distillation [36], adversarial training [35], [39], [40], adversarial detection [22], [37], [38], and input reconstruction [41][42]. However, to the best of our knowledge, no defense method was demonstrated to be effective against all adversarial attacks [44][50]. In particular, adversarial examples will always exist since none of the trained DNNs are perfect. Therefore, adversarial defense in FDIA detection mainly aims to degrade the attack performance and increase the attack cost.

In this section, we first review several state-of-the-art adversarial defense mechanisms proposed in the literature. We analyze these approaches and show that they have inherent limitations to mitigate adversarial attacks in FDIA detection effectively. We verify our analysis with simulations in Section VI. After that, we propose our random input padding framework to train adversarial-resilient DNNs for FDIA detection. The evaluation in Section VI shows that our framework can significantly decrease the overall performance of adversarial attacks.

A. State-of-the-Art Methods

1) **Defensive Distillation:** Neural network distillation was first proposed to reduce the size of DNN architectures [51]. In 2016, Papernot *et al.* employed distillation as an adversarial defense approach in the computer vision field [36]. The basic idea behind DNN distillation is to transfer the knowledge from a trained model to a new model. [36] first trained a DNN F with the original datasets $\{X, Y\}$. After that, a second DNN F^d that has the same structure as F was trained with the new labeled dataset $\{X, F(X)\}$, in which $F(X)$ is the probability vector produced by the last softmax layer of $F(X)$. The new DNN F^d is shown to be less sensitive to input perturbations and then becomes more robust to adversarial attacks.

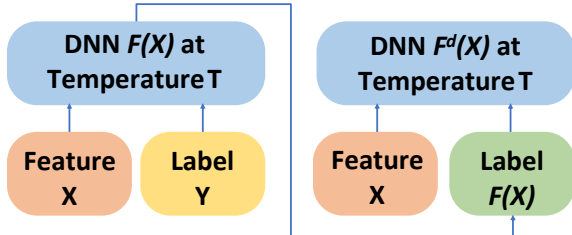


Fig. 2: Basic structure of defensive distillation [36].

Limitation Analysis: The defensive distillation method shows excellent performance against several typical adversarial attacks in the computer vision domain [36]. However, a common

premise of adversarial attacks in the computer vision domain is that the size of the perturbation needs to be relatively small so that the adversarial pictures will not be noticed by human eyes. The attacker in [36] iteratively generates adversarial perturbation and stops when the number of perturbed features is larger than a threshold. The assumption on perturbation size is no longer feasible in adversarial attacks to DNN-based FDIA detection. For example, if there is a reckless attacker who aims to inject considerable false data to the state estimation, and she/he only needs to focus on the size of the total injected false data $\hat{\mathbf{a}}$. Although model distillation decreases the DNN's sensitivity to input perturbations, the attacker can still iteratively search for a valid adversarial measurement \mathbf{z}_{adv} that deceives the DNN model without considering the size of \mathbf{v} . Therefore, model distillation is not capable to defend against adversarial attacks in FDIA detection tasks. Defensive distillation has been shown to be vulnerable to C&W attack in 2017 [49]. In Section VI, we will demonstrate it is also vulnerable to our attack proposed in Algorithm 1.

2) **Adversarial Training:** Adversarial training is one of the common methods to mitigate an adversarial attack [35], [39], [40]. The basic principle of adversarial training is to generate and include adversarial examples in each data batch during the training stages. As the DNN is trained to recognize adversarial examples, it becomes more robust.

Limitation Analysis: Adversarial training needs to generate adversarial examples for each batch of data during the training process, which increases the training computation overhead significantly. As demonstrated by line 9 in Algorithm 1, to avoid being removed by the residual-based detection scheme, the adversarial perturbations need to be projected to fit the constraint. The mapping process will further significantly introduce computation overhead to the adversarial training process. Therefore, adversarial training is not scalable to large systems that contain massive data resources. Meanwhile, [35] shows that adversarial training can increase the robustness of DNNs for single-step attacks but perform deficiently for iterative attacks, which make it inappropriate for FDIA detection (Algorithm 1 performs an iterative attack).

3) **Adversarial Detection:** Adversarial detection aims to recognize adversarial examples at the DNN inference stage [22], [37], [38]. In particular, an auxiliary binary classification DNN F_{adv} is trained with normal records and corresponding adversarial examples [22] to detect if an input is an adversarial example. The adversarial detection DNN F_{adv} will be employed first to recognize the input records, and only the normal records will be fed into the original functional DNN. The structure of employing adversarial detection in FDIA can be illustrated by Fig. 3.

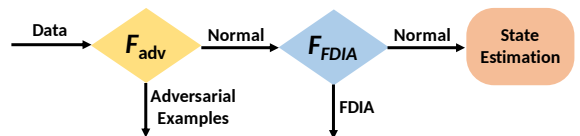


Fig. 3: Basic structure of adversarial detection in FDIA.

Limitation Analysis: A common assumption of adversarial

detection is that the adversarial examples follow a different distribution from normal inputs. The assumption is reasonable in the computer vision domain (the natural images will not contain the well-crafted perturbations) but not applicable for FDIA detection. As introduced in Section IV, the manifold of the injected false data \mathbf{a} can be represented by the constraint $\mathbf{B}\mathbf{a} = \mathbf{0}$ empirically. To bypass the built-in residual-based detection of state estimation, the total injected false data $\hat{\mathbf{a}}$ is also required to meet the constraint $\mathbf{B}\hat{\mathbf{a}} = \mathbf{0}$. Since the number of the possible attack scenarios (different meters can be compromised) can be large, intuitively, the crafted adversarial measurement vector \mathbf{z}_{adv} shares a similar manifold with the false measurement vector \mathbf{z}_a in the FDIA detection. In fact, \mathbf{z}_{adv} can be considered as special \mathbf{z}_a . Therefore, adversarial detection will not work effectively in FDIA detection tasks. This analysis can also be adapted to input reconstruction methods [41][42]. Adversarial detection is also vulnerable to dynamic and iterative attacks [22][41][42].

B. Random Input Padding Framework

As discussed above, the adversarial defense in DNN-based FDIA detection is non-trivial since the adversarial measurements share the same manifold as the general false measurements. Given the victim model, the attacker generates the perturbation \mathbf{v} for \mathbf{z}_a iteratively through a gradient-based optimization process. As presented in [35], the perturbation generated by multi-step attacks usually has worse transferability, which indicates that adversarial perturbation \mathbf{v} in FDIA detection is highly likely to be unique for each given \mathbf{z}_a . Therefore, there is an intuition that the perturbation will no longer work if the input to the model changes. Inspired by the stochastic-based defense mechanisms in the computer vision field [42][43], we propose a random input padding defense framework to mitigate the effect of adversarial attacks in FDIA detection.

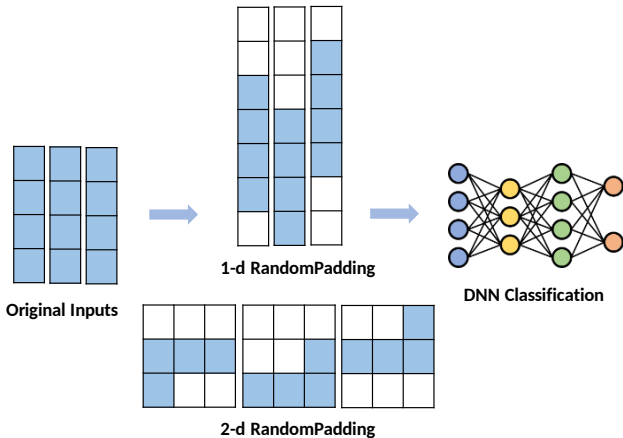


Fig. 4: Illustration of random inputs padding framework. Each record in the plain inputs is a 4-d vector. The above 1-d padding scheme randomly pads four zeros to plain inputs and the padded vectors become an 8-d ($P = 8$). The below 2-d padding scheme reshapes the inputs pads five zeros, which finally generates 3×3 dimensional records ($P = 9$).

The philosophy of our random input padding framework is straightforward, and the overall structure is shown in Fig 4. A random padding layer is added in front of the DNN in both training and inference stages. In general, the measurements of the sensors \mathbf{z} are used as the features to train the detection models. Our framework firstly requires the operator to pick a padding dimension number P ($P > m$) as the input feature numbers for the DNN. Thereafter, we pad $P - m$ zeros randomly to the plain inputs \mathbf{z} and there will be $P - m$ padding scenarios in total. The DNN is then required to learn the pattern from the plain measurements that are embedded into the padded inputs during the training process. During the inference stage, when a new measurement vector \mathbf{z} is received, the framework randomly pads \mathbf{z} to a P dimensional vector and feeds the padded vector to the DNN. Ideally, the detection rate against adversarial attacks should be $1 - \frac{1}{P-m+1}$ ($P \geq m$). The padding framework also works with possible input reshape, as shown in Fig 4.

As the padding process is random for each \mathbf{z} at the inference stage, the attacker (and even the operator) cannot know the final DNN padded input vectors even when she/he knows the whole framework. The attacker will be able to generate perturbations for one of the $P - m$ padding scenarios. Since the multi-steps perturbations have relatively weak transferability, the adversarial attacks should have a lower success rate under the random padding framework. Intuitively, a larger P will decrease the success rate of adversarial attacks and finally increase the robustness of the DNN used for FDIA detection.

Different from [43], our framework requires input data pre-processing (padding) during the training stage and cannot be applied to a trained model directly. This is because the measurement data of a specific power system should follow the manifold defined by the physical property of the system, which will be destroyed if the measurement vectors are reshaped, resized, or sampled directly. On the other hand, the FDIA detection performance of the legitimate data vector \mathbf{z} and false measurements \mathbf{z}_a will not be constrained by the padding/scale size if an appropriate structure of the neural network is selected. Meanwhile, our framework only increases the computation of the training process slightly and is compatible with different neural networks.

VI. SIMULATION

In this section, we first evaluate the effect of adversarial attacks in DNN-based FDIA detection. After that, we evaluate the state-of-the-art adversarial defense approaches discussed in Section V-A and verify our analysis on their limitation through numeric simulations. Finally, we evaluate the performance of our random padding framework.

Synthetic Dataset Generation: The simulations are conducted based on the standard IEEE 118-bus system, which was used as a test benchmark in previous literature [1], [7], [9], [11], as shown in Fig. 5. We employ the MATPOWER [53] tool to derive the \mathbf{H} matrix of the system and simulate the power flow measurement data of each branch as \mathbf{Z} . In our evaluation, each measurement vector \mathbf{z} contains $m = 186$ measurements. The FDIA attack is also implemented with

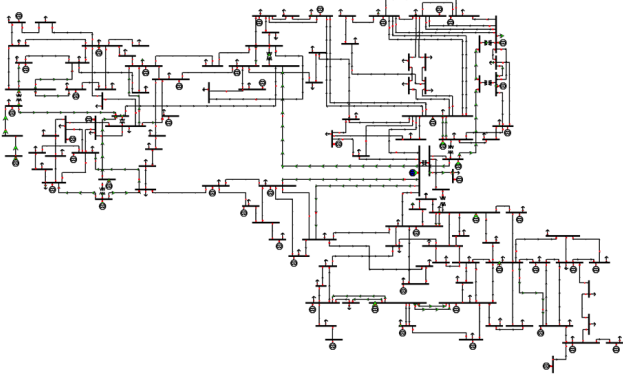


Fig. 5: IEEE 118-Bus system [52].

MATLAB based on the corresponding \mathbf{H} . We simulate a dataset D_{train} that contains 30,000 legitimate measurement vectors. We pollute half of the records in D_{train} by injecting false data generated by the FDIA. In order to simulate practical possible attacks, we set different compromised number $70 < k < 100$ and the indexes of the compromised measurements are randomly selected. The legitimate measurement records (unpolluted) in D_{train} are labeled as Normal (0) and false measurement data records as False (1). Meanwhile, it is straightforward that a larger false noise \mathbf{a} will endow the false measurements a more clear pattern, which is easier for DNNs to learn. To evaluate the performance of the trained DNN, we consider and generate small \mathbf{a} whose L_1 -Norm follows a Gaussian distribution with the mean equal to 5% of the mean of the legitimate measurements' L_1 -Norm. In addition to D_{train} , we generate four test datasets. We consider the scenarios that there are 75, 80, 85, 90 measurements being compromised by the attacker respectively and simulate 1000 polluted (false) data for each scenario. The indexes of the compromised measurements of each scenario are randomly selected.

Target DNN: We train a feed-forward neural network F as the target DNN in our simulations, and the structure of F is shown in Table II. We randomly split D_{train} into training part and testing part, with the test part contains 15% of records in D_{train} . We employ the categorical cross-entropy as the loss function and utilize stochastic gradient descent to optimize the loss. Through tuning parameters, F finally achieves a 98.9% detection accuracy and 98.6% recall. F is developed with the Tensorflow and Keras library. The simulations are conducted on a Windows 10 machine with an Intel i7 CPU and an additional NVIDIA GeForce GTX 1070 GPU to accelerate the training process.

TABLE II: Model Structure of F

Layer	1	2	3	4	5	6
Nodes	186	128	64	16	0.25 Dropout	2 Softmax

* Dense layer is used for each layer.

* The activation function is *ReLU* unless specifically noted.

Evaluation Metrics: The evaluation metrics of adversarial

attacks can be different according to the attack purpose. In this work, we set three metrics to evaluate the attack performance in this study. The first metric is the detection **Recall** of the target DNN under adversarial attacks, which indicates the probability of the adversarial measurements to bypass the DNN detection. In addition, we consider two different attack scenarios. The first attack scenario happens when the attacker aims to inject a specific false vector \mathbf{a} into state estimation, such as to gain specific profit through modifying local marginal price [54], [55]. In this scenario, the size of perturbation \mathbf{v} is required to be small. Therefore, our second metric is the L_2 -Norm of \mathbf{v} of effective adversarial measurements that successfully bypass the DNN detection. We note this metric as **Bias L_2 -Norm**. The second attack scenario is that a malicious attacker aims to inject considerable false data to the state estimation and the size of $\hat{\mathbf{a}}$ is expected to be large. We set the L_2 -Norm of $\hat{\mathbf{a}}$ to be the third evaluation metric, which is noted as **Valid L_2 -Norm** in this paper. In summary, from the attacker's point of view, a lower Recall, a smaller Bias L_2 -Norm, and a larger Valid L_2 -Norm indicate a more successful adversarial attack and vice versa.

A. Adversarial Attacks in FDIA Detection

This subsection studies the vulnerabilities of DNN through adversarial attacks. As described above, the size of the simulated FDIA noise in D_{train} follows a Gaussian distribution. Therefore, it is intuitive that a larger injected false data \mathbf{a} will result in a higher probability to be detected by F . On the contrary, the false measurements \mathbf{z}_a become difficult to be distinguished by F if \mathbf{a} is small, but the FDIA performance also becomes worse.

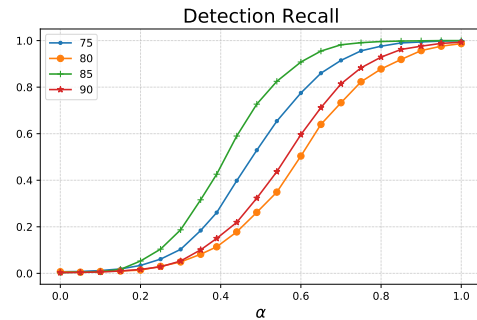


Fig. 6: Vanilla attack recall.

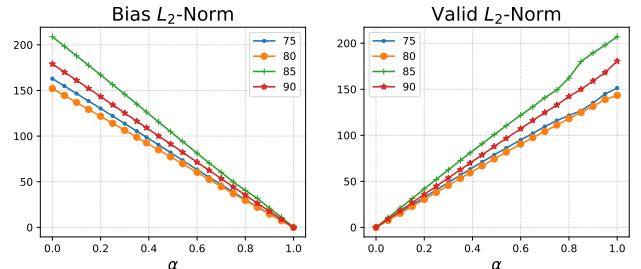


Fig. 7: Vanilla attack bias.

Baseline: To demonstrate the effectiveness of adversarial attacks, we set a vanilla attack as a baseline. The vanilla attack will simply multiple the injected false data \mathbf{a} with a factor α in the four test datasets, and the newly crafted false measurements are fed into F for evaluation. The evaluation results of vanilla attack are shown in Fig. 6 and Fig. 7 respectively. As analyzed, from Fig. 6 we can learn that a larger α will result in a higher detection recall of the false measurements, and the detection performance may be various for different attack scenarios. Fig. 7 demonstrates that the trend of Bias L_2 -Norm and Valid L_2 -Norm of the vanilla attack is adverse with the α increases under vanilla attack. Overall, if the vanilla attacker aims to obtain a relatively higher probability to bypass the F detection, she/he obtain a high Bias L_2 -Norm and low Valid L_2 -Norm.

We then evaluate the performance of adversarial attacks with Algorithm 1, as summarized in Table III. The evaluation demonstrates that the adversarial attacks can decrease the detection recall significantly with a relatively low bias L_2 -Norm and high valid L_2 -Norm. The attack performance can be various for different attack scenarios and slightly affected by the attack parameters (*size*). By comparing Table III with Fig. 6 and Fig. 7, we can learn that the adversarial attacks significantly out-performs vanilla attacks.

TABLE III: Attack Performance of Plain DNN

Case	Size	Recall	Bias L_2 -Norm	Valid L_2 -Norm
75	0.1	3.9%	79.7	112.2
	0.5	0.9%	87.2	111.29
	1.0	1.9%	89.6	108.9
80	0.1	18.9%	64.5	114.4
	0.5	12.9%	76.7	117.5
	1.0	10.9%	80.2	114.1
85	0.1	7.0%	115.2	134.4
	0.5	3.9%	124.0	134.3
	1.0	3.9%	127.0	131.4
90	0.1	12.9%	79.7	165.5
	0.5	3.9%	109.9	178.0
	1.0	5.9%	109.9	178.0

B. State-of-the-art Defense Methods

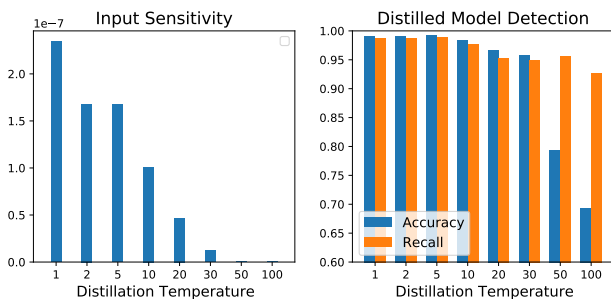


Fig. 8: Distilled DNNs performance.

1) *Defensive Distillation:* Similar to [36], we select different distillation temperatures (1, 2, 5, 10, 20, 30, 50, 100) to train the corresponding distilled DNN models. Fig. 8

demonstrates the properties of the distilled models. The left figure in Fig. 8 shows that the input sensitivity decreases when the temperature increase, which coordinates with the effect of distillation, and the DNN models become less sensitive to input perturbation. From the right figure, we can learn that there is a slight decrease in both detection accuracy and recall of the distilled models with the temperature increases. However, when the temperature becomes larger, such as larger than 50, the detection accuracy decreases significantly, which indicates a high false-positive rate.

We evaluate the performance of distilled DNNs under adversarial attacks, as shown in Table IV. The detection recall was low in most attack cases and the bias L_2 -Norm and valid L_2 -norm are comparable with plain DNN. Overall, model distillation presents ineffective defense performance to adversarial attacks in FDIA detection.

TABLE IV: Attack Performance of Distilled DNNs

Temp	Case	Recall	Bias L_2 -Norm	Valid L_2 -Norm
1	75	2.9%	77.2	116.8
	80	57.9%	209.1	212.5
	85	49.0%	207.0	248.7
	90	23.9%	149.1	225.1
2	75	3.9%	154.2	185.1
	80	27.0%	104.2	185.5
	85	34.9%	186.4	242.5
	90	3.9%	94.9	156.1
5	75	1.0%	90.5	108.6
	80	5.9%	84.6	126.1
	85	0.41%	195.8	148.9
	90	27.0%	158.6	252.1
10	75	5.9%	97.2	140.1
	80	10.9%	71.2	144.0
	85	43.0%	241.0	295.8
	90	7.9%	96.4	190.8
20	75	2.0%	57.6	139.5
	80	12.9%	91.57	155.6
	85	20.0%	145.1	175.4
	90	34.9%	179.2	271.6
30	75	15.9%	94.6	157.8
	80	11.9%	73.8	157.4
	85	47.9%	203.7	222.3
	90	41.9%	196.2	213.4
50	75	38.9%	172.9	233.8
	80	28.9%	123.2	193.2
	85	43.0%	215.1	212.4
	90	40.0%	202.1	268.0
100	75	20.0%	136.2	196.1
	80	18.0%	102.1	181.6
	85	36.0%	201.7	230.9
	90	10.9%	74.6	202.0

* Parameters: *size* = 0.1.

2) *Adversarial Training:* We follow the method described in [56] to implement the adversary training. During each training epoch, we generate the adversarial measurements of the mini-batch measurement data with the real-time trained DNN and label them as false. We then add the generated adversarial measurements to the mini-batch data and train the model. Meanwhile, we project the generated measurements to follow the linear constraints defined by Equation (5). Fig. 9 shows the training loss and detection accuracy during adversarial training.

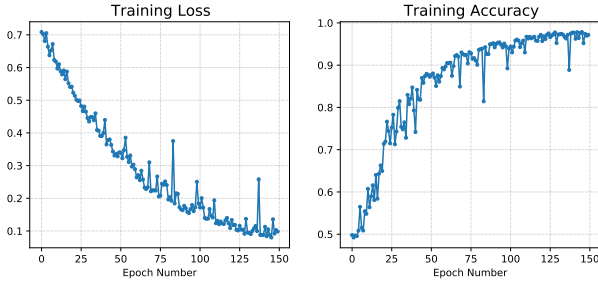


Fig. 9: Adversarial training process.

As analyzed in Section V-A2, the projection process significantly increases the training computation overload, which makes it impractical to be employed in large-scale power systems. In our evaluation, the training process takes around 650 seconds to converge and achieves 96.5% overall detection accuracy. For comparison, the normal training process takes around 10 seconds to converge in the same computer.

TABLE V: Attack Performance of Adversarial Training

Case	Size	Recall	Bias L_2 -Norm	Valid L_2 -Norm
75	0.1	15%	96.2	103.9
	0.5	7.0%	115.8	113.8
	1.0	5.9%	122.8	115.8
80	0.1	43.1%	147.1	1.53
	0.5	45.7%	359.9	354.4
	1.0	47.2%	640.8	635.1
85	0.1	63.9%	142.0	167.5
	0.5	61.0%	471.8	437.5
	1.0	62.9%	519.0	678.3
90	0.1	62.2%	187.6	231.2
	0.5	66.4%	761.8	768.4
	1.0	69.3%	1485.9	1495.7

We evaluate the defense performance of adversarial training, we launched our adversarial attacks to the trained model, and the results are summarized in Table V. In our simulations, overall, adversarial training is demonstrated to increase the robustness of DNN to a certain degree. The detection recall of the adversarial trained DNN is higher than plain DNN in all evaluation scenarios. Meanwhile, although the Valid L_2 -Norm values are very large in some scenarios (**Case 90**), the corresponding Bias L_2 -Norm values are also large. However, for **Case 75**, the defense performance is still limited.

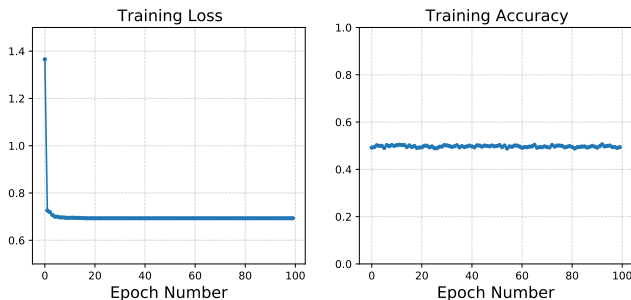


Fig. 10: Training process of the auxiliary f_{adv} for adversarial detection.

3) *Adversarial Detection*: We employ the adversarial detection methods described in [22] and generate the adversarial measurements of all the false measurements in D_{train} . We use the false measurements and their corresponding adversarial measurements to train a binary auxiliary classification DNN F_{adv} . We empirically attempt different structures and parameters of the F_{adv} and observe that its performance is not reliable and the training process does not converge. As analyzed in Section V-A3, we explain that this result is caused by the similar manifolds shared between the false measurements \mathbf{z}_a and the adversarial measurements \mathbf{z}_{adv} . Fig. 10 provides the training process of an example F_{adv} in our simulation.

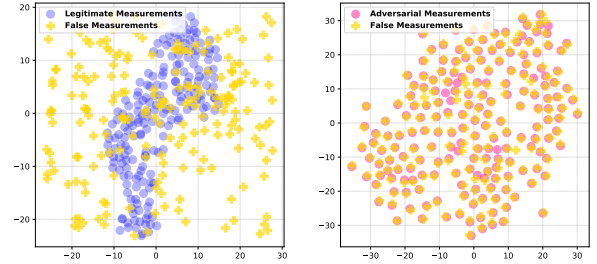


Fig. 11: The manifolds of legitimate measurements, false measurements and adversarial measurements with t-SNE dimensionality reduction.

To verify our analysis, we utilize the t-Distributed Stochastic Neighbor Embedding (t-SNE) to visualize the manifolds in 2-dimensions, as shown in Fig. 11. From the left figure, we can learn that the false measurements follow different manifolds with the legitimate measurements. This explains the effectiveness of DNN-based FDIA detection and the high detection recall of F . From the right figure, however, we can learn that the manifolds between the false measurements and corresponding adversarial measurements are very similar (overlapping markers). This phenomenon is caused by the physical property of the power system and the constraints defined by Equation (5). The adversarial measurements \mathbf{z}_{adv} can be regarded as special false measurements. Therefore, adversarial detection can not distinguish the adversarial measurements from the DNN's inputs effectively in FDIA detection.

C. Random Input Padding Framework

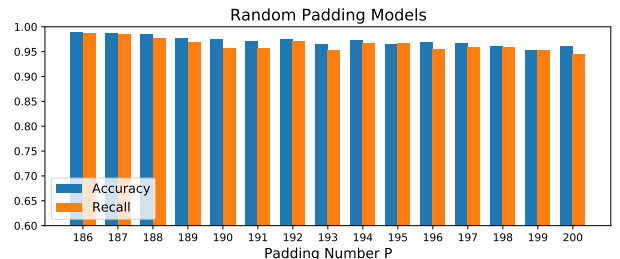


Fig. 12: Detection performance of random input padding DNNs.

We evaluate the defense performance of our framework based on F and modify the number of the input neurons

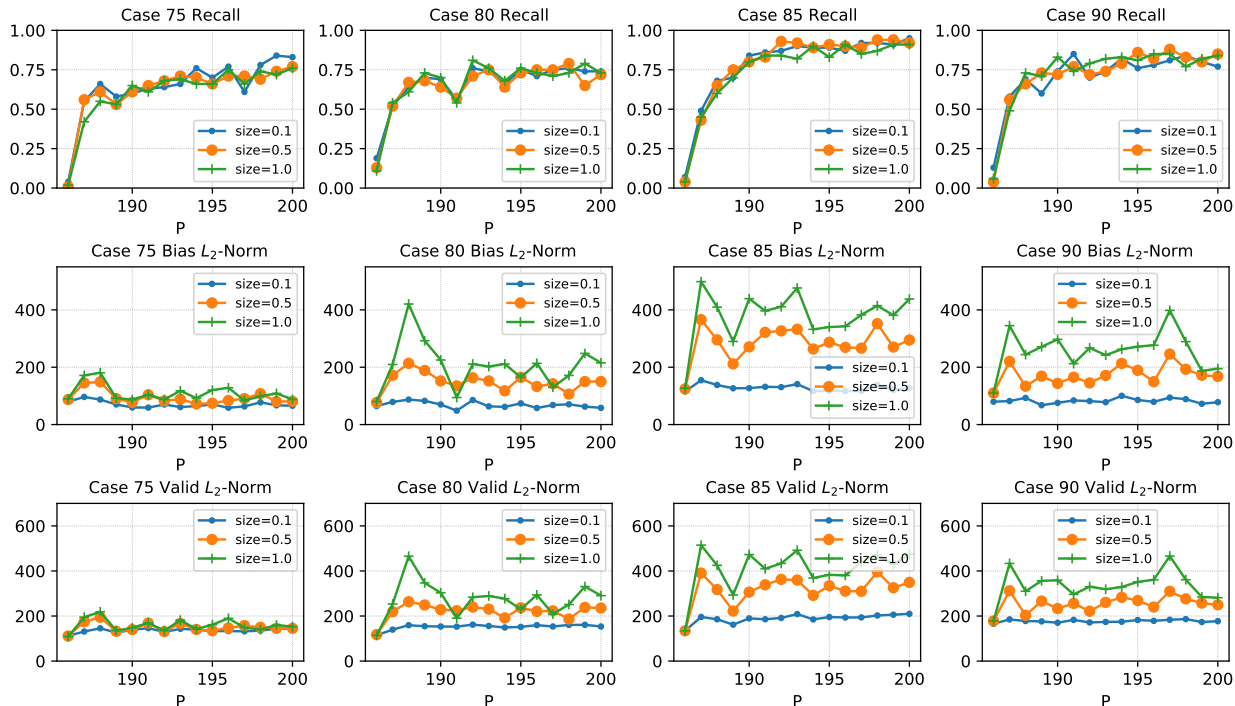


Fig. 13: Adversarial evaluation of random input padding DNNs.

according to the padding number P for F . The overall detection performance of padded DNNs are shown in Fig. 12. We can learn that with the padding number P increases, the detection accuracy of DNN decreases gradually and becomes stable. The detection accuracy and recall of the padded DNNs reach around 96% and 95% respectively. Fig. 12 shows that the random padding framework only slightly decreases the FDIA detection performance, compared with the plain models ($P = 186$). Our framework pads zeros in front of and/or after the plain measurements, which will not destroy the pattern of normal inputs.

Figure. 13 shows the defense performance of the random input padding framework under different adversarial attacks. The top four figures in Fig. 13 present the detection recall of the padded DNNs. The detection recalls of all attack scenarios increase remarkably when the padding number is relatively small ($P = 187, 188$). After that, the detection recalls increase gradually and will converge to a specific range with the padding number increases. We can observe that the detection recalls under different attack scenarios do not strictly follow the expected $1 - \frac{1}{(P-186)+1}$ ($P \geq 186$) regulation. We note this is due to the transferability of adversarial measurements under different padding cases. Overall, we can observe that the padding framework significantly increases the resiliency of DNNs against adversarial attacks.

The bottom eight figures in Fig. 13 demonstrate the bias L_2 -Norm and valid L_2 -Norm of the adversarial attacks. In general, we can observe that the bias L_2 -Norm follows a similar trend with valid L_2 -Norm. Compared with the plain DNN, our

random padding framework can increase the bias L_2 -Norm, which can decrease the performance of FDIA that targets local marginal price. On the contrary, similar to adversarial training, the valid L_2 -Norm can also be large in some test scenarios. This phenomenon indicates that the attacker may inject considerable noise into the state estimation. However, our framework maintains a high detection recall under all test scenarios, which makes it outperform the other typical defensive methods discussed in this paper.

VII. DISCUSSION AND FUTURE WORK

As we discussed in Section V, currently, there is no defense mechanism that is robust to all adversarial attacks. In general, adversary examples/measurements will always exist since the DNN is imperfect and an attacker can always modify the input to force the DNN to change the prediction output. For example, if the vanilla attacker in Section VI-A sets the factor α to a small value, the resulted false measurements will have a high probability to bypass the DNN's detection. In this paper, we note the attacker can generate his/her adversarial perturbations based on multiple padding cases to increase their transferability and finally bypass the random padding system, as used in [57] and [20]. However, generating transferable perturbations will affect the attack performance, such as the valid L_2 -Norm, and increase labor and resources of the attacker [20].

We proposed the input padding framework for FDIA detection in this paper and the framework is compatible with different models. Inspired by the randomly-selected autoencoder scheme in [42], we believe our framework can be used

together with their system to further increase the DNNs' robustness in FDIA detection. In the future, we will study the implementation and performance of this joint system.

In DNN-based FDIA detection, in addition to decreasing the detection recall, we expect the defense mechanism to increase the bias L_2 -Norm and decrease the valid L_2 -Norm. In our simulations, the random padding framework increases both the bias L_2 -Norm and the valid L_2 -Norm (similar to adversarial training). We consider this as an open problem in our future work and will study defense methods that achieve satisfying performance in all three metrics.

VIII. CONCLUSION

The adversarial attacks present a serious threat to DNN-based FDIA detection. In this paper, we study the defense mechanism of adversarial attacks in FDIA and methods to increase the robustness of corresponding DNN models. We first analyze the unique properties of adversarial attack and defense in FDIA detection and summarize the defense requirements. We evaluate several state-of-the-art defense methods and demonstrate that they have intrinsic limitations for this task through analysis and numeric simulations. After that, we propose a random padding framework for employing DNNs in FDIA detection. The framework is compatible with different DNNs and introduces little extra computation. Evaluation results present that our framework outperforms the typical defense mechanisms and can significantly increase the robustness of DNNs against adversarial measurements in FDIA detection. Meanwhile, the framework will hardly decrease DNNs' detection performance on the normal inputs.

REFERENCES

- [1] Y. Liu, P. Ning, and M. K. Reiter, "False data injection attacks against state estimation in electric power grids," in *Proceedings of the 16th ACM conference on Computer and communications security*, pp. 21–32, 2009.
- [2] M. A. Rahman and H. Mohsenian-Rad, "False data injection attacks with incomplete information against smart power grids," in *2012 IEEE GLOBECOM*, pp. 3153–3158, IEEE, 2012.
- [3] Z.-H. Yu and W.-L. Chin, "Blind false data injection attack using pca approximation method in smart grid," *IEEE Transactions on Smart Grid*, vol. 6, no. 3, pp. 1219–1226, 2015.
- [4] X. Liu, Z. Li, X. Liu, and Z. Li, "Masking transmission line outages via false data injection attacks," *IEEE Transactions on Information Forensics and Security*, vol. 11, no. 7, pp. 1592–1602, 2016.
- [5] S. Bi and Y. J. Zhang, "Defending mechanisms against false-data injection attacks in the power system state estimation," in *2011 IEEE GLOBECOM Workshops (GC Wkshps)*, pp. 1162–1167, IEEE, 2011.
- [6] Q. Yang, D. An, R. Min, W. Yu, X. Yang, and W. Zhao, "On optimal pmu placement-based defense against data integrity attacks in smart grid," *IEEE Transactions on Information Forensics and Security*, vol. 12, no. 7, pp. 1735–1750, 2017.
- [7] M. Ozay, I. Esnaola, F. T. Y. Vural, S. R. Kulkarni, and H. V. Poor, "Machine learning methods for attack detection in the smart grid," *IEEE transactions on neural networks and learning systems*, vol. 27, no. 8, pp. 1773–1786, 2015.
- [8] J. Yan, B. Tang, and H. He, "Detection of false data attacks in smart grid with supervised learning," in *2016 International Joint Conference on Neural Networks (IJCNN)*, pp. 1395–1402, IEEE, 2016.
- [9] Y. He, G. J. Mendis, and J. Wei, "Real-time detection of false data injection attacks in smart grid: A deep learning-based intelligent mechanism," *IEEE Transactions on Smart Grid*, vol. 8, no. 5, pp. 2505–2516, 2017.
- [10] Q. Deng and J. Sun, "False data injection attack detection in a power grid using rnn," in *IECON 2018-44th Annual Conference of the IEEE Industrial Electronics Society*, pp. 5983–5988, IEEE, 2018.
- [11] J. James, Y. Hou, and V. O. Li, "Online false data injection attack detection with wavelet transform and deep neural networks," *IEEE Transactions on Industrial Informatics*, vol. 14, no. 7, pp. 3271–3280, 2018.
- [12] A. Ayad, H. E. Farag, A. Youssef, and E. F. El-Saadany, "Detection of false data injection attacks in smart grids using recurrent neural networks," in *2018 IEEE ISGT*, pp. 1–5, IEEE, 2018.
- [13] M. Ashrafuzzaman, Y. Chakhchoukh, A. A. Jillepalli, P. T. Tosic, D. C. de Leon, F. T. Sheldon, and B. K. Johnson, "Detecting stealthy false data injection attacks in power grids using deep learning," in *2018 14th IWCNC*, pp. 219–225, IEEE, 2018.
- [14] X. Niu, J. Li, J. Sun, and K. Tomsovic, "Dynamic detection of false data injection attack in smart grid using deep learning," in *2019 IEEE Power & Energy Society Innovative Smart Grid Technologies Conference (ISGT)*, pp. 1–6, IEEE, 2019.
- [15] C. Wang, S. Tindemans, K. Pan, and P. Palensky, "Detection of false data injection attacks using the autoencoder approach," *arXiv preprint arXiv:2003.02229*, 2020.
- [16] Y. Chen, Y. Tan, and D. Deka, "Is machine learning in power systems vulnerable?," in *2018 IEEE SmartGridComm*, pp. 1–6, IEEE, 2018.
- [17] Y. Chen, Y. Tan, and B. Zhang, "Exploiting vulnerabilities of load forecasting through adversarial attacks," in *Proceedings of the Tenth ACM International Conference on Future Energy Systems*, pp. 1–11, 2019.
- [18] J. Tian, T. Li, F. Shang, K. Cao, J. Li, and M. Ozay, "Adaptive normalized attacks for learning adversarial attacks and defenses in power systems," in *2019 IEEE SmartGridComm*, pp. 1–6, IEEE, 2019.
- [19] J. Li, Y. Yang, and J. S. Sun, "Searchfromfree: Adversarial measurements for machine learning-based energy theft detection," in *2020 IEEE International Conference on Communications, Control, and Computing Technologies for Smart Grids (SmartGridComm)*, pp. 1–6, IEEE, 2020.
- [20] J. Li, Y. Yang, J. S. Sun, K. Tomsovic, and H. Qi, "Conaml: Constrained adversarial machine learning for cyber-physical systems," *arXiv preprint arXiv:2003.05631*, Accepted by the 16th ACM ASIA Conference on Computer and Communications Security (ACM ASIACCS 2021), 2020.
- [21] T. Liu and T. Shu, "Adversarial false data injection attack against nonlinear ac state estimation with ann in smart grid," in *International Conference on Security and Privacy in Communication Systems*, pp. 365–379, Springer, 2019.
- [22] J. H. Metzen, T. Genewein, V. Fischer, and B. Bischoff, "On detecting adversarial perturbations," *arXiv preprint arXiv:1702.04267*, 2017.
- [23] C. Jiongcong, G. Liang, C. Zexiang, H. Chunchao, X. Yan, L. Fengji, and Z. Junhua, "Impact analysis of false data injection attacks on power system static security assessment," *Journal of Modern Power Systems and Clean Energy*, vol. 4, no. 3, pp. 496–505, 2016.
- [24] M. Khalaf, A. Hooshyar, and E. El-Saadany, "On false data injection in wide area protection schemes," in *2018 IEEE PESGM*, pp. 1–5, 2018.
- [25] R. B. Bobba, K. M. Rogers, Q. Wang, H. Khurana, K. Nahrstedt, and T. J. Overbye, "Detecting false data injection attacks on dc state estimation," in *Preprints of the First Workshop on Secure Control Systems, CPSWEEK*, vol. 2010, 2010.
- [26] S. Bi and Y. J. Zhang, "Graphical methods for defense against false-data injection attacks on power system state estimation," *IEEE Transactions on Smart Grid*, vol. 5, no. 3, pp. 1216–1227, 2014.
- [27] T. T. Kim and H. V. Poor, "Strategic protection against data injection attacks on power grids," *IEEE Transactions on Smart Grid*, vol. 2, no. 2, pp. 326–333, 2011.
- [28] J. Chen and A. Abur, "Placement of pmus to enable bad data detection in state estimation," *IEEE Transactions on Power Systems*, vol. 21, no. 4, pp. 1608–1615, 2006.
- [29] G. Liang, J. Zhao, F. Luo, S. R. Weller, and Z. Y. Dong, "A review of false data injection attacks against modern power systems," *IEEE Transactions on Smart Grid*, vol. 8, no. 4, pp. 1630–1638, 2016.
- [30] R. Deng, G. Xiao, R. Lu, H. Liang, and A. V. Vasilakos, "False data injection on state estimation in power systems—attacks, impacts, and defense: A survey," *IEEE Transactions on Industrial Informatics*, vol. 13, no. 2, pp. 411–423, 2016.
- [31] C. Szegedy, W. Zaremba, I. Sutskever, J. Bruna, D. Erhan, I. Goodfellow, and R. Fergus, "Intriguing properties of neural networks," *arXiv preprint arXiv:1312.6199*, 2013.
- [32] I. J. Goodfellow, J. Shlens, and C. Szegedy, "Explaining and harnessing adversarial examples," *arXiv preprint arXiv:1412.6572*, 2014.
- [33] A. Rozsa, E. M. Rudd, and T. E. Boulton, "Adversarial diversity and hard positive generation," in *Proceedings of the IEEE CVPR Workshops*, pp. 25–32, 2016.

- [34] S.-M. Moosavi-Dezfooli, A. Fawzi, and P. Frossard, "Deepfool: a simple and accurate method to fool deep neural networks," in *Proceedings of the IEEE CVPR*, pp. 2574–2582, 2016.
- [35] A. Kurakin, I. Goodfellow, and S. Bengio, "Adversarial machine learning at scale," *arXiv preprint arXiv:1611.01236*, 2016.
- [36] N. Papernot, P. McDaniel, X. Wu, S. Jha, and A. Swami, "Distillation as a defense to adversarial perturbations against deep neural networks," in *2016 IEEE Symposium on Security and Privacy (SP)*, pp. 582–597, IEEE, 2016.
- [37] S. Ma and Y. Liu, "Nic: Detecting adversarial samples with neural network invariant checking," in *Proceedings of the 26th NDSS*, 2019.
- [38] W. Xu, D. Evans, and Y. Qi, "Feature squeezing: Detecting adversarial examples in deep neural networks," *arXiv preprint arXiv:1704.01155*, 2017.
- [39] A. Shafahi, M. Najibi, M. A. Ghiasi, Z. Xu, J. Dickerson, C. Studer, L. S. Davis, G. Taylor, and T. Goldstein, "Adversarial training for free!," in *Advances in Neural Information Processing Systems*, pp. 3353–3364, 2019.
- [40] F. Tramèr, A. Kurakin, N. Papernot, I. Goodfellow, D. Boneh, and P. McDaniel, "Ensemble adversarial training: Attacks and defenses," *arXiv preprint arXiv:1705.07204*, 2017.
- [41] S. Gu and L. Rigazio, "Towards deep neural network architectures robust to adversarial examples," *arXiv preprint arXiv:1412.5068*, 2014.
- [42] D. Meng and H. Chen, "Magnet: a two-pronged defense against adversarial examples," in *Proceedings of the 2017 ACM CCS*, pp. 135–147, 2017.
- [43] C. Xie, J. Wang, Z. Zhang, Z. Ren, and A. Yuille, "Mitigating adversarial effects through randomization," in *International Conference on Learning Representations*, 2018.
- [44] H. Xu, Y. Ma, H.-C. Liu, D. Deb, H. Liu, J.-L. Tang, and A. K. Jain, "Adversarial attacks and defenses in images, graphs and text: A review," *International Journal of Automation and Computing*, vol. 17, no. 2, pp. 151–178, 2020.
- [45] G. Liang, S. R. Weller, J. Zhao, F. Luo, and Z. Y. Dong, "The 2015 ukraine blackout: Implications for false data injection attacks," *IEEE Transactions on Power Systems*, vol. 32, no. 4, pp. 3317–3318, 2016.
- [46] "Ieee standard for synchrophasor measurements for power systems," *IEEE Std C37.118.1-2011 (Revision of IEEE Std C37.118-2005)*, pp. 1–61, 2011.
- [47] N. Papernot, P. McDaniel, S. Jha, M. Fredrikson, Z. B. Celik, and A. Swami, "The limitations of deep learning in adversarial settings," in *2016 IEEE EuroS&P*, pp. 372–387, IEEE, 2016.
- [48] A. Madry, A. Makelov, L. Schmidt, D. Tsipras, and A. Vladu, "Towards deep learning models resistant to adversarial attacks," *arXiv preprint arXiv:1706.06083*, 2017.
- [49] N. Carlini and D. Wagner, "Towards evaluating the robustness of neural networks," in *2017 IEEE Symposium on Security and Privacy (SP)*, pp. 39–57, IEEE, 2017.
- [50] A. Athalye, N. Carlini, and D. Wagner, "Obfuscated gradients give a false sense of security: Circumventing defenses to adversarial examples," in *International Conference on Machine Learning*, pp. 274–283, PMLR, 2018.
- [51] G. Hinton, O. Vinyals, and J. Dean, "Distilling the knowledge in a neural network," *arXiv preprint arXiv:1503.02531*, 2015.
- [52] I. C. for a Smarter Electric Grid, "IEEE 118-Bus System." <https://icseg.iti.illinois.edu/ieee-118-bus-system/>. [Online; accessed 16-Jan-2021].
- [53] R. D. Zimmerman, C. E. Murillo-Sánchez, and R. J. Thomas, "Matpower: Steady-state operations, planning, and analysis tools for power systems research and education," *IEEE Transactions on power systems*, vol. 26, no. 1, pp. 12–19, 2010.
- [54] S. Bi and Y. J. Zhang, "False-data injection attack to control real-time price in electricity market," in *2013 IEEE Global Communications Conference (GLOBECOM)*, pp. 772–777, IEEE, 2013.
- [55] L. Xie, Y. Mo, and B. Sinopoli, "False data injection attacks in electricity markets," in *2010 First IEEE International Conference on Smart Grid Communications*, pp. 226–231, IEEE, 2010.
- [56] A. Kurakin, I. Goodfellow, and S. Bengio, "Adversarial examples in the physical world," *arXiv preprint arXiv:1607.02533*, 2016.
- [57] S.-M. Moosavi-Dezfooli, A. Fawzi, O. Fawzi, and P. Frossard, "Universal adversarial perturbations," in *Proceedings of the IEEE CVPR*, pp. 1765–1773, 2017.